Environ Earth Sci (2015) 73:3801–3817
DOI 10.1007/s12665-014-3665-z

ORIGINAL ARTICLE

Freshwater resource characterization and vulnerability to climate change of the Shela aquifer in Lamu, Kenya

Cornelius Okello · Marco Antonellini · Nicolas Greggio · Nina Wambiji

Received: 4 December 2013 / Accepted: 26 August 2014 / Published online: 14 September 2014

Abstract Salinization of coastal groundwater systems causes a severe deterioration both in amount and quality of fresh groundwater resources. To support the sustainable use and management of fresh groundwater, quantification and characterization of these coastal resources are important in view of the population growth anticipated in many African countries. Analytical methods were used to determine: (1) the shape and volume of the freshwater lens, (2) the elevation of the water table, (3) the depth of the freshwater/saltwater interface in the Shela aquifer, and (4) the expected change of volume resulting from change of recharge and sea level rise driven by climate change. The results of the analytical modelling have shown that the average hydraulic conductivity is 0.755 m/d, the average water table elevation is 2 m above sea level and the average depth of the freshwater/saltwater interface is -80 m.a.s.l. The volume of the aquifer is $\approx 124 \times 10^6$ m^3 when discharge from the Shela well field is factored in. Climate change is expected to have an impact on the recharge and ultimately the aquifer's volume; under the A1b conditions, the volume is expected to increase to 199×10^6 m^3 whereas in the A2 scenario it is expected to decrease to 27×10^6 m^3. The saltwater intrusion indicator M for today's conditions (0.004) decreases to 0.5 M in the A1b scenario by 2100 whilst it increases to 24.9 M in the A2 scenario for the same time period, indicating an extremely higher vulnerability to saltwater intrusion in the latter scenario. A simple linear correlation with the expected population growth of 1.25 million people by 2050 shows the aquifer failing as a water source by 2033.

Keywords Analytical solutions · Groundwater · Saltwater intrusion · Vulnerability · Climate change

C. Okello · M. Antonellini · N. Greggio
IGRG (Integrated Geoscience Research Group), University of Bologna, Via San Alberto 128, 48100 Ravenna, Italy

C. Okello (✉)
University of Cadiz, Polígono San Pedro s/n, Aulario Norte, Puerto Real, 11519 Cadiz, Spain
e-mail: cbokello@gmail.com

N. Wambiji
Kenya Marine and Fisheries Research Institute, P.O. Box 81651-80100, Mombasa, Kenya

Introduction

Coastlines around the world are home to a large percentage of the world's population. Water resources in these regions are, therefore, subject to intensive stresses and demands from both natural and human drivers (Cartwright et al. 2004). Coastal aquifers constitute an important source of freshwater supply and are often confronted with the problem of saltwater intrusion (Lobo Ferreira et al. 2007). The proximity of coastal aquifers to saltwater creates unique groundwater sustainability issues, because of the strong influence of the salinity gradient between salty sea water and fresh coastal groundwater (Roeper et al. 2013). Many coastal aquifers in the world are currently experiencing intensive saltwater intrusion caused by both natural and man-induced processes (Custodio 2010). Furthermore, the demand for fresh groundwater resources is expected to rise due to future population growth leading to higher vulnerability of fresh groundwater supply (Essink 2001). Availability of freshwater resources in the coastal zones in the future will further be challenged by the trends of climate change that predict higher temperatures and lower rainfall (Giupponi and Mordechai 2003) that may enhance the

drought in the dry periods and the precipitation in the wet periods (IPCC 2007). These changes in climatic conditions will result in sea level rise and low freshwater heads, which are important components influencing saltwater intrusion in coastal areas.

Vulnerability in this instance is defined as the propensity of saltwater intrusion to occur and is defined both for "current conditions" (i.e. for a given set of hydrogeological parameters) and for anticipated changes in aquifer stress (Werner et al. 2012). Salinization of groundwater systems leads to a severe deterioration of the quality and quantity of existing fresh groundwater resources in coastal aquifers making saltwater intrusion a major contributor to coastal groundwater vulnerability. Whilst saltwater intrusion is a natural process within coastal groundwater, and bound to occur, it becomes an environmental problem when excessive pumping of freshwater from an aquifer takes place as this accelerates the process and brings it out of the natural equilibrium (Soni and Pujari 2010; Wirojanagud and Charbeneau 1985; Reilly and Goodman 1987; Saeed et al. 2002; Werner et al. 2009). When the freshwater/saltwater system is in natural equilibrium, a pumping well located in the freshwater zone can disturb this equilibrium. This results in the saltwater moving upwards towards the well as it tries to reach hydrostatic equilibrium in a phenomenon known as saltwater up-coning (Reilly and Goodman 1987). Furthermore, in situations where there is not enough freshwater recharge from rainfall and the hydraulic conductivity is large, there may not be enough freshwater to counteract the hydraulic pressure of the surrounding saltwater and salinization will occur (Barlow and Reichard 2010; Mollema et al. 2013a, b).

Changes in climate variables can also significantly alter groundwater recharge rates, affecting the availability of fresh groundwater (Ranjan et al. 2006). The Intergovernmental Panel on Climate Change (IPCC) developed four different long-term emissions storylines (Special Reports on Emissions Scenario (SRES)) to represent the range of driving forces that have been widely used in the analysis of possible climate change, its impacts, and options to mitigate climate change. For each storyline, several different scenarios were used to examine the possible outcomes arising from a range of models that use similar assumptions about driving forces (IPCC 2000). The A1 storyline describes a future world of very rapid economic growth and global population that peaks in mid-century and declines thereafter, and the rapid introduction of new and more efficient technologies. The A1b scenario represents a balance across all energy sources with no heavy reliance on one particular one. It describes a very heterogeneous world where the underlying theme is self-reliance and preservation of local identities. It is further characterized by continuously increasing population, primarily regionally oriented and per capita economic development as well as slower and fragmented technological change compared to other storylines (IPCC 2007). According to IPCC (2001), African countries are more vulnerable to these changes due to lack of institutional capacity and economic development. However, current research has mainly focused on surface water and very little is known about the potential impacts on groundwater (Nyenje and Batelaan 2009; Kebede et al. 2010). As there is very limited knowledge about the impacts of climate change and its coastal-related issues on Africa on a continental scale and at country level, little has been done to assess these issues (Zinyowera et al. 1998; Desanker et al. 2001; Brown et al. 2009).

If coastal aquifers are to be used as operational reservoirs of water resources, development of tools that facilitate the prediction of the behaviour of coastal aquifers under different stressors and assessment of their vulnerability are required (Ranjan et al. 2009). This concept of groundwater vulnerability to saltwater intrusion is the basis for the evaluation of the risk of groundwater contamination from salinity and in the development of management options to preserve the quality of groundwater resources (Kattaa et al. 2010). To support the sustainable use of fresh groundwater for coastal communities, quantification and characterization of coastal groundwater resources are necessary within the framework of Integrated Coastal Zone Management (Ranjan et al. 2009). This requires knowledge of local hydrological and geological controls which are connected to the dynamics of salinity gradients (Roeper et al. 2013). The lateral and vertical extent of the freshwater lenses is determined by these controls such as the hydraulic parameters of the sediments (hydraulic conductivity, porosity), water table elevation, density difference between freshwater and seawater, seasonal and tidal flooding, and amount of groundwater recharge (i.e. Harris 1967; Fetter 1972; Collins and Easley 1999; Anderson et al. 2000; Schneider and Kruse 2005). In the absence of these data, which is a common occurrence particularly in developing countries, a feasible option is to attempt to provide estimates of the depth of the freshwater/saltwater interface in both coastal and oceanic island settings using analytical solutions.

Some basic hydrogeological knowledge of the aquifer and the water budget is required to use these analytical solutions effectively. The shape of the steady-state interface between fresh and saline groundwater is one of the canonical problems of hydrogeology (Maas 2007). Salt and freshwater are separate stratified water bodies in an aquifer (Haubold 1975). Typically, the water density differences between saltwater and freshwater produce a sloping freshwater/saltwater interface, whereby deeper saltwater is overlain by freshwater (Barlow 2003; Mollema and Antonellini 2013; Werner and Simmons 2009). The position of

this interface along coastlines was first studied by Badon-Ghijben (1888, 1889) and Herzberg (1901) who came up with the Ghyben–Herzberg relationship used to this day (Soni and Pujari 2012). Many other analytical solutions have since been developed for particular cases and even more numerical models have been used to simulate the complex hydrogeological situations in specific sites (Langevin et al. 2005; Essink et al. 2010; Schneider and Kruse 2005; Vandenbohede et al. 2011; Bobba et al. 2000; Mollema and Antonellini 2013). Although analytical solutions normally cannot describe complex "real-world" problems because of their simplified physical assumptions and geometry, they do serve other very important purposes. They provide hydro-geologists an understanding of the hydrodynamic trends of flow in aquifers and fundamental insights on the physical processes at work. Despite their simplified assumptions, feasibility studies can employ analytical solutions as reliable tools in first-cut engineering and hydrologic analyses. These solutions are used to perform preliminary calculations based on basic information and simplified assumptions before using more sophisticated models that require hydrological and hydrogeological information that is either unavailable or not known (Bear et al. 1999). In this study, analytical solutions have been used, given the limited hydrological and hydrogeological data available for the Shela aquifer. They give a first approximation of the depth of the fresh and saltwater interface that allows for the estimation of the freshwater lens size and how water abstraction for human use from wells affects the freshwater lens.

The main aim of this study is to define and characterize (1) the size and total volume of the freshwater lens (2) the elevation of the water table, (3) the depth of the freshwater/saltwater interface of the Shela aquifer, and (4) the expected change in volume under the influence of climate change considering recharge and sea level rise variations for the Intergovernmental Panel on Climate Change (IPCC) A1b and A2 SRES (IPCC 2007). It is emphasized that the purpose of this study is to take a first step towards understanding and quantifying the size and shape of the freshwater lens under the sand dunes lying between Shela and Kizingoni/Kipungani. The study will provide a base for future studies in Lamu and may be useful for other locations around the world with limited information.

Study area

The Lamu Island (Fig. 1) is an island cast into the Indian Ocean off the Kenyan coast located between LAT 2°24′ S and LAT 2°34′ S and between LONG 40°81′ E and LONG 40°92′ E. It has a total land surface of about 50 km^2. Of this, about 19 km^2 is covered by a double row of longitudinal sand dunes located along the entire length of the southern coastline. The 3-km-wide Kizingoni dunes are located to the southwest of the island south of the Kipunguni settlement. The dunes wedge out eastwards and narrow to 700 m at the Shela area in the southeast. The dunes have a height ranging from 20 to 65 m and are almost entirely covered with fine–medium grained Pleistocene carbonate sands as well as loamy sands and pink-coral limestone sediments (Kuria 2008). The area is underlain by sand, silt, and silty clays deposits as well as by weathered to fresh corals which are in turn overlaid by coral breccia (Scott 2011). The mild dune relief combined with the good infiltration capacity of the sandy soil at the top increases the amounts of vertical recharge and prevents surface run-off (Archer 2012; Kuria 2008). The Lamu Island has no rivers and groundwater recharge is derived from local precipitation and infiltration processes. The broad and rugged terrain that lies between the rows of the sand dunes is the most important recharge feature in the area that acts as a water drainage basin where all surface run-off systems infiltrate and percolate to augment the underlying aquifer, which is able to store freshwater that is harvested for domestic use (Scott 2011). The entire catchment area is well drained evidenced by its hydrology, which is largely dominated by infiltration and no surface run-off systems (Kuria 2008). The rest of the island beyond the sand dunes is covered with a thick blanket of poorly drained clayey sands (Republic of Kenya 1991). This, combined with the presence of dense perennial thickets and palm trees scattered over the island and mangrove forests along the northern shore (Republic of Kenya 2012a), further reduces the infiltration from the landward side of the dunes as perennial vegetation has been found to decrease water infiltration rates (Peng et al. 2004) (Fig. 2).

The unconfined Shela aquifer lies underneath these sand dunes and serves as the primary source of water for the entire island. The ground water is extracted from 30 partial penetrating wells in the eastern part of the unconfined aquifer ranging from 6 to 16 m deep (Kuria 2008). The water table slopes gently towards the ocean at a gradient of about 0.001–0.005. The recent establishment and development of the beach resorts together with a very substantial population increase have adversely reduced the recharge area of the aquifer catchment (Kuria 2008). Lamu is the site for Kenya's second harbour that is currently under construction and is expected to tremendously increase the demand on this already over-exploited freshwater source.

The study area lies along the equatorial coastal climatic zone characterized by two monsoon winds. The climate is generally warm with average precipitation (P) of 83 mm annually and has two distinct rainy seasons: the long rain period between March and May with an average of 151.9 mm and the short rain period from mid-October to mid-December with an average of 56.5 mm [figures

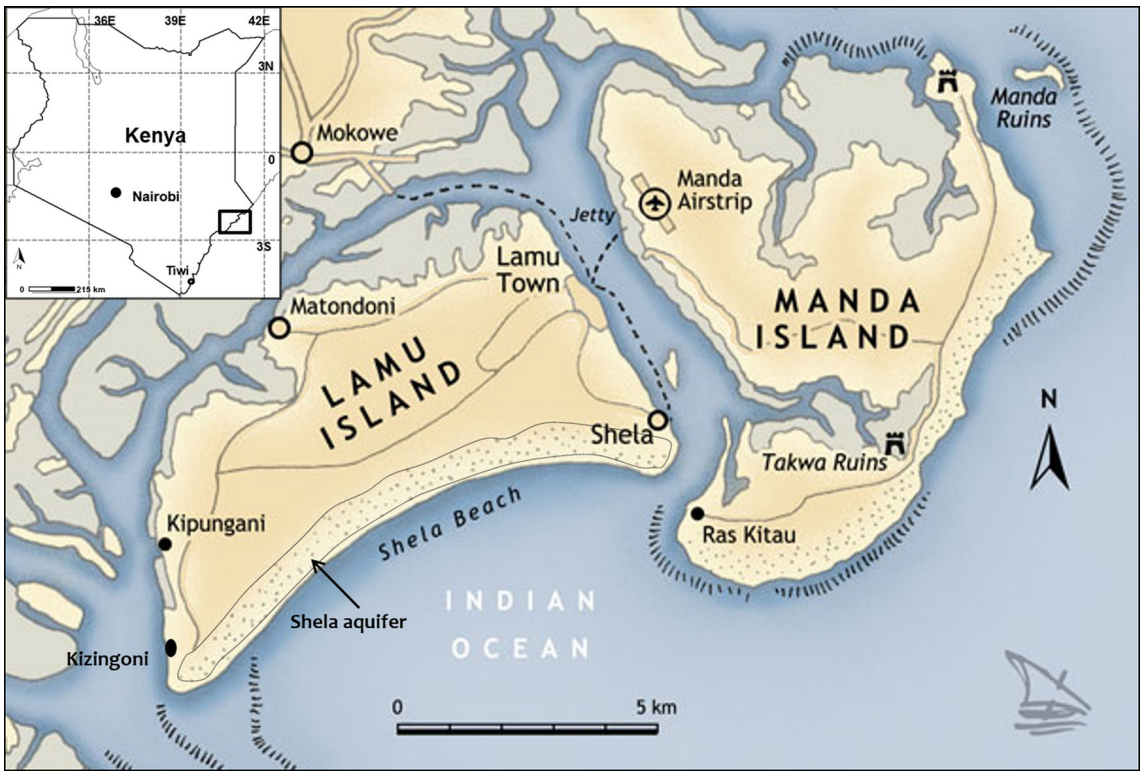

Fig. 1 Map showing the location of the unconfined part of the Shela aquifer under the sand dunes south of Lamu Island, Kenya (adapted and modified from http://www.theafricanaviationtribune.com/2013/01/kenya-pics-look-at-lamus-manda-airstrip.html)

calculated from data provided by the Kenya Meteorological Department (KMD)]. The temperatures are usually high ranging between 23 and 33 °C. The hottest months are from December to April whilst the coldest are from May to July (Fig. 3). The mean annual potential evapotranspiration (PET) is high, 2,257 mm per year. Precipitation data from KMD were for the time period of 1960–2012 whilst the temperature data were from 1974 to 2012.

The population of Lamu Island currently stands at just over 22,000 with the main economic activities being tourism and small-scale subsistence farming. Lamu Water and Sewerage Company (LAWASCO), a governmental organization in charge of water provision in Lamu, estimates that each person consumes 0.06 m^3 of water a day. The Republic of Kenya (RoK) through the Ministry of Transport has already started construction of the port at Manda Bay (North–Northeast of Manda Island, Fig. 1). This port is part of a larger project which plans to establish a transport corridor of road, rail, and pipeline linking the proposed port of Lamu through Northern Kenya to South Sudan and Ethiopia (ESIA 2013). According to the Republic of Kenya (2011), the port is expected to be functional by 2030 and to perform at its peak by 2050. A new metropolis will be established in Lamu along with a highway, railway system and an airport. Large ranches will also be established to support mechanized agriculture. In this scenario, the population of Lamu is expected to grow to 1.25 million people by 2050 (Republic of Kenya 2011).

Methods

The Shela aquifer was divided into 23 equal topographic transects 500 m apart using ArcGIS and digital elevation maps obtained from the USGS website (http://gdex.cr.usgs.gov/gdex/). The profile line at the centre of the aquifer (profile 10) was used as the reference point for the calculations performed because (a) it passes right through the middle of the aquifer dissecting it into two roughly equal parts, (b) one of the wells in the Shela well field (well no. 30) is found at the mid-point of the profile line, and (c) it aligns with one of the tomography lines by Kuria (2008), therefore, there is information about the freshwater lens at this point.

The A1b scenario was selected as it represents a balanced, optimistic outlook on climate change whilst the A2 scenario was selected because present climate data show an inclination towards this scenario. The monthly total withdrawals of water for all 30 wells were provided by

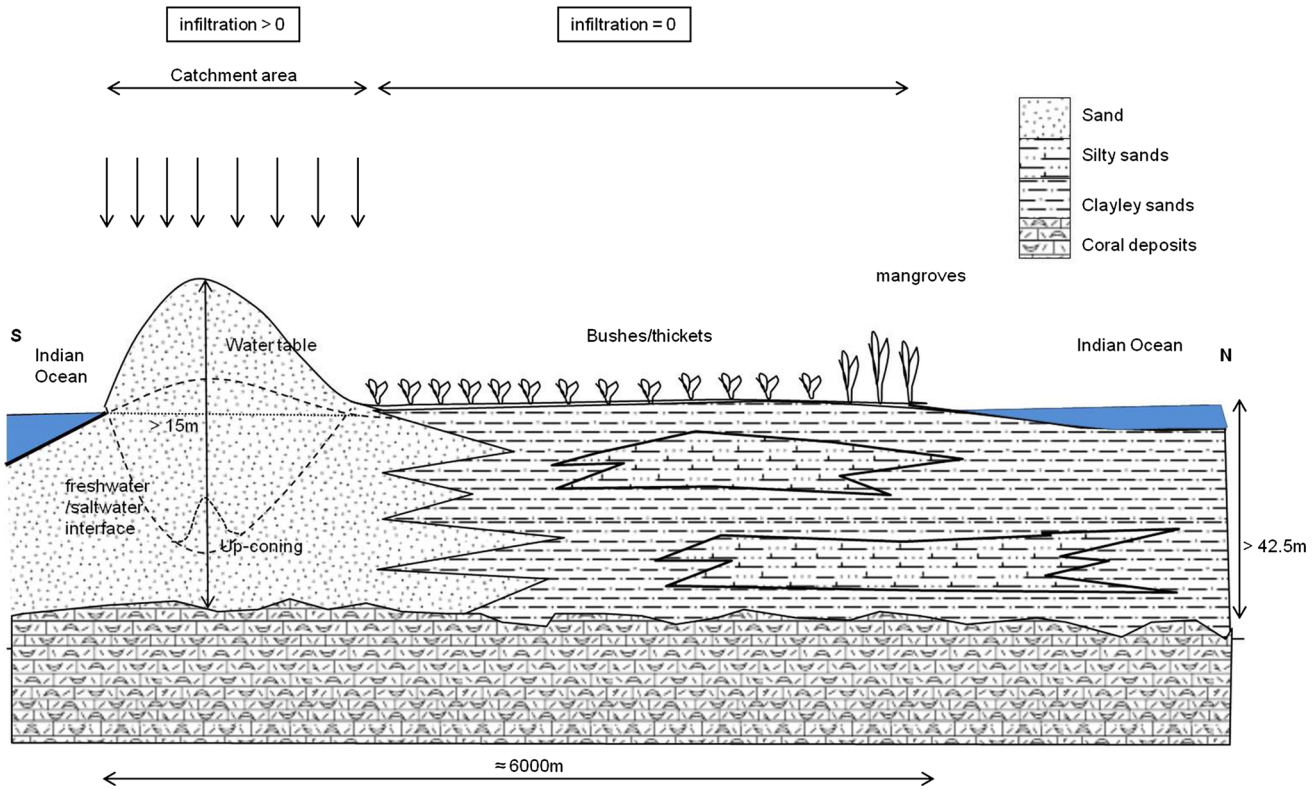

Fig. 2 A sketch representation of the N–S cross-section through the centre of the Lamu Island showing the stratigraphy and lithology of the study area

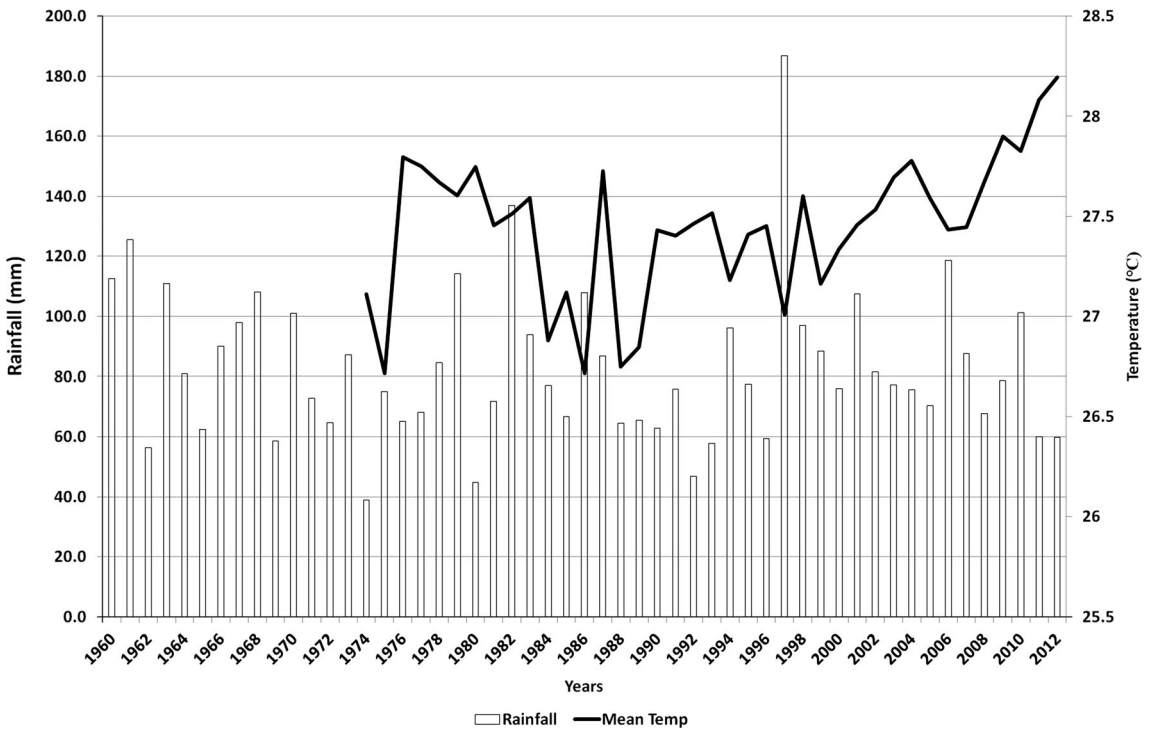

Fig. 3 Historical series of annual averages of rainfall and temperature for Lamu from 1960 to 2012 (KMD)

LAWASCO and daily averages per well were calculated by dividing the total abstraction by the number of wells as specific data on the discharge per each well was not available.

Calculations of the theoretical size of the freshwater lens below sand dunes

The Dupuit–Ghyben–Herzberg analytical formula is derived from the continuity equation, Darcy's Law, the Ghyben–Herzberg relationship, and the Dupuit assumptions of horizontal flow (Bear 1972). This formula is used to derive the position of the water table and saltwater interface in island freshwater lenses (defined as a single body of fresh groundwater that extends across the island and is separated from the underlying saltwater by a single, sharp, continuous interface). This relationship utilizes the island's geometry, the hydraulic conductivity (K) of the aquifer, and the potential recharge (w) (Fetter 1972). The Dupuit–Ghyben–Herzberg equation has been solved with the boundary condition assumption that the water table and interface meet at the shoreline. It has been used to derive the steady-state position of the water table and interface through an island that is assumed to be of infinite length. The infinite island strip corresponds to the dune system overlying the Shela aquifer, which is elongated along the shoreline. "Infinite strip" implies that the K, w, island width, and head distribution do not vary significantly along the long dimension of the island. Therefore, any cross-island section normal to the shoreline is representative of the configuration of the lens (Vacher 1988).

The thickness of the freshwater lens in a homogenous aquifer is a function of its width (R), position with respect to the centre of the island (r), K, the density ratio of fresh and saltwater (G), and w (Budd and Vacher 1991). The main assumption in this study is that the aquifer is homogeneous. The horizontal and vertical K are assumed to be equal, the saltwater is at rest, there is a sharp interface with a negligible mixing zone, the annual recharge is uniform, and therefore, the lens is in a steady-state. The water storage in the vadose zone is assumed to be negligible because of the high permeability of the sand in the dunes and the prevailing climatic conditions (high temperatures). Little information is known about the landward side of the aquifer beyond the sand dunes.

The methodology below was used to model only the catchment area of the aquifer that follows the outline of the sand dunes.

Determining the hydraulic conductivity of the aquifer

The K was determined using the Fetter Infinite-Strip Island Solution (Fetter 1972)

$$h^2 = \frac{w[R^2 - (R-r)^2]}{K(1+G)} \quad (1)$$

by solving the equation for K using a known h

$$K = \frac{w[R^2 - (R-r)^2]}{h^2(1+G)} \quad (2)$$

where

$$G = \left(\frac{\rho_f}{\rho_s - \rho_f}\right)$$

ρ_s (1.032 g/cm^3) and ρ_f (1 g/cm^3) are the densities of Indian Ocean's saltwater and freshwater, respectively.

The water table elevation data, h, were obtained from a combination of well depth data, the water column in the well from Kuria (2008), and the use of ArcGIS and digital elevation maps (DEMs). The elevation of the sand dunes at the location of well at profile line 10 (Fig. 4) was established using the DEMs for Lamu in ArcGIS. The water column value was subtracted from the well depth. The result was then subtracted from the sand dune elevation to obtain the height of the water table.

The PET and P data for a 10-year series were obtained from New LocClim, a local climate estimator developed by FAO (2002). The PET was then subtracted from the P to obtain the potential recharge. The months with a P–PET value larger than zero (May and June as seen in Fig. 5) were considered to be the months where recharge of the aquifer was occurring. These months' average was then calculated to obtain the annual recharge. The daily potential recharge was derived by dividing the annual recharge by the number of days in a year.

By entering these data in Eq. (2) it was possible to calculate K.

Determining water table elevation for all profiles

Once the K was determined, the Fetter Infinite-Strip Island Solution Eq. (1) was used to determine the elevation of the water table (h_f) along the other profile lines (Fig. 5).

Computing the freshwater/saltwater interface

The freshwater/saltwater interface depth (ξ) was expressed by the Ghyben–Herzberg relationship

$$\xi = \left(\frac{\rho_f}{\rho_s - \rho_f}\right) h_f \approx 31.25\, h_f \quad (3)$$

Volumetric calculations

The integral volume of a section slice with a thickness of 500 m through the aquifer was computed by taking the surface integral above sea level for the water table

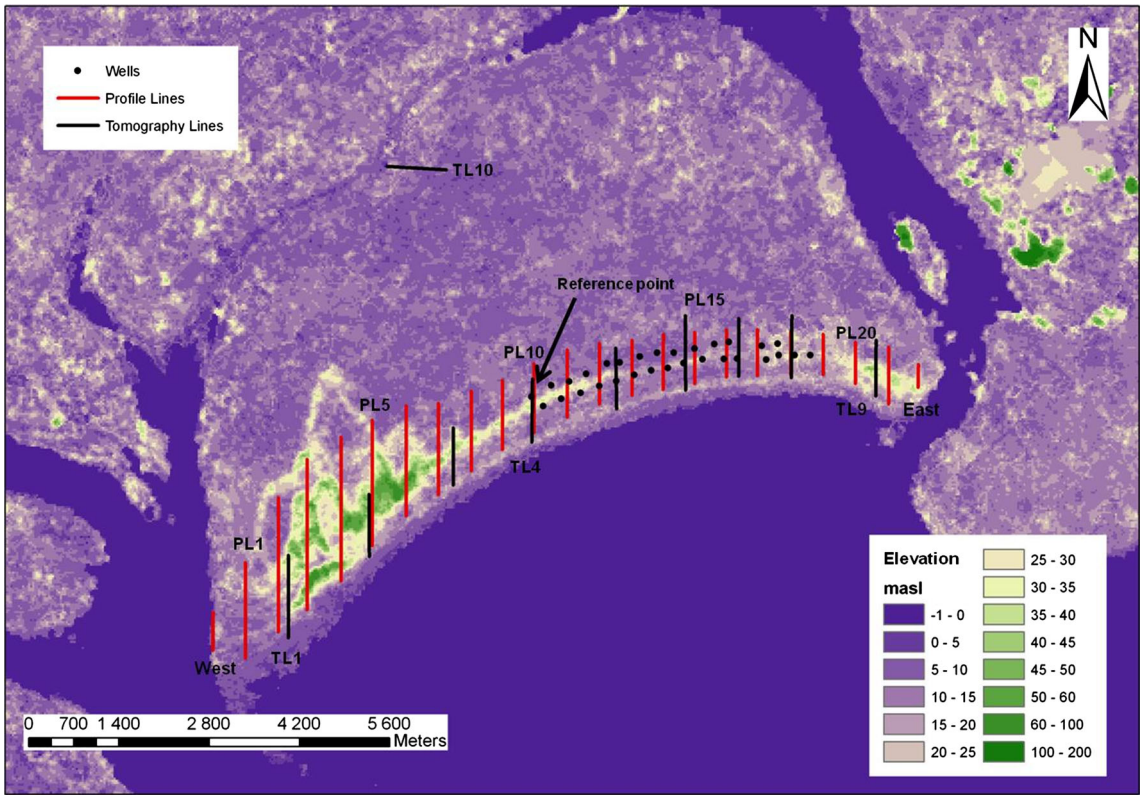

Fig. 4 A DEM of Lamu Island showing the elevation of sand dunes and the profile lines used for this study (volume profiles) in relation to the position of the tomography lines by Kuria (2008)

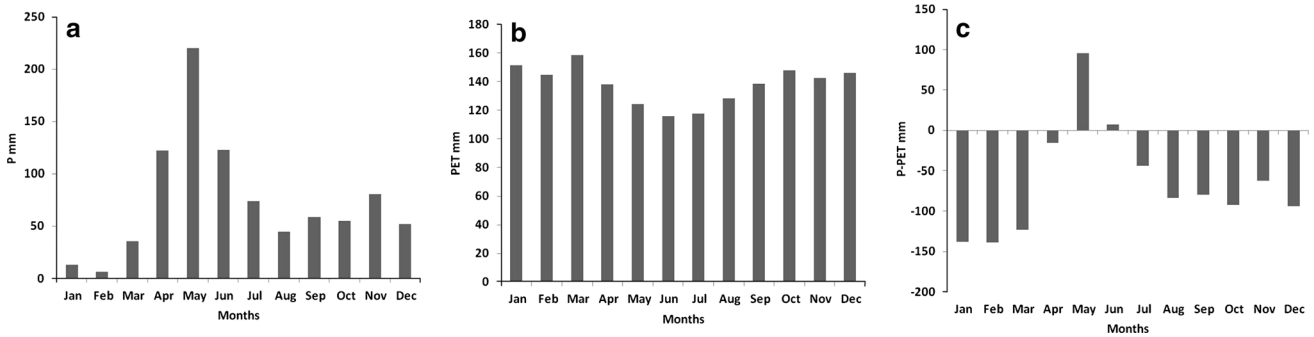

Fig. 5 Graphs showing the 10-year average monthly P (**a**) and PET (**b**) as well as the values for P–PET (**c**)

elevation and below sea level for the depth of the freshwater/saltwater interface (Beyer 2013). The two surface integrals were added and multiplied by 500 m to obtain the volume of the slice (Fig. 6).

The water table surface is obtained from

$$S_{\mathrm{h}} = \sqrt{\frac{w}{k(1+G)}} \int_0^{2a} \sqrt{2\mathrm{ar} - r^2}\,\mathrm{d}r$$

and the freshwater/saltwater surface is obtained from

$$S_z = G\sqrt{\frac{w}{k(1+G)}} \int_0^{2a} \sqrt{2\mathrm{ar} - r^2}\,\mathrm{d}r$$

The exact solutions of these integrals are

$$S_{\mathrm{h}} = \frac{\pi a^2}{4}\sqrt{\frac{w}{k(1+G)}}$$

for the water table surface, and

$$S_z = \frac{G\pi a^2}{4}\sqrt{\frac{w}{k(1+G)}}$$

for the freshwater/saltwater interface surface.

The total freshwater aquifer area becomes

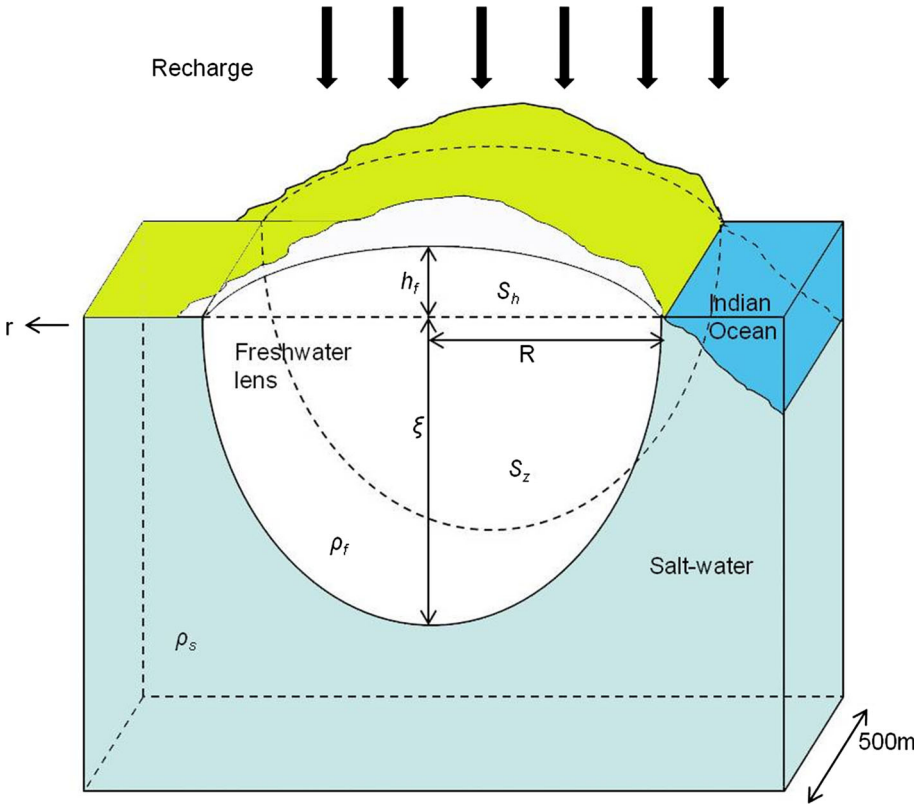

Fig. 6 Sketch representation of a cross-section with 500 m width through the Shela aquifer showing freshwater lens overlain by sand dunes

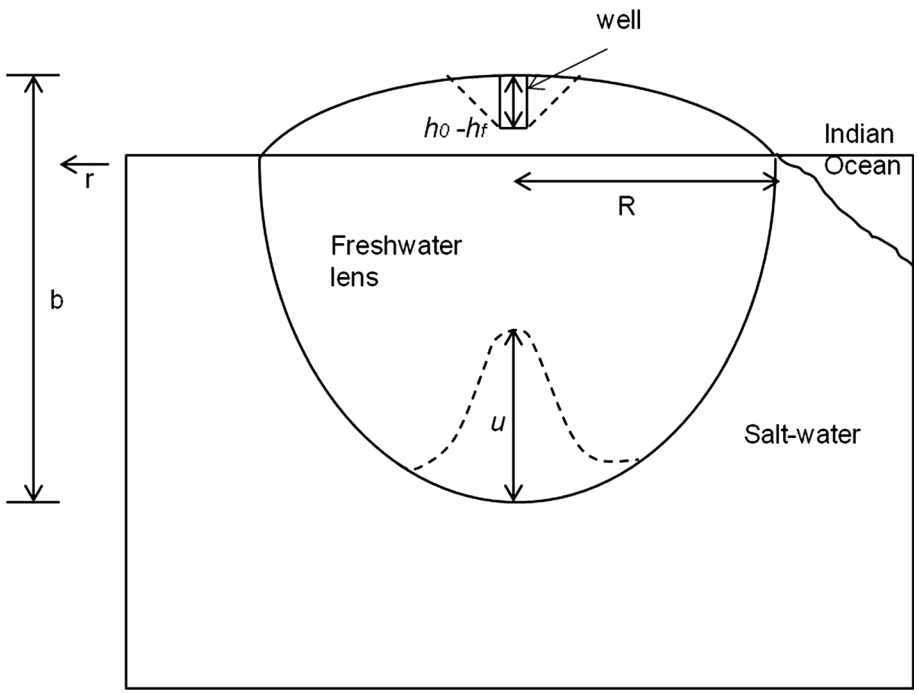

Fig. 7 Sketch representation of a cross-section through the Shela aquifer showing drawdown and up-coning that results from abstraction from a pumping well

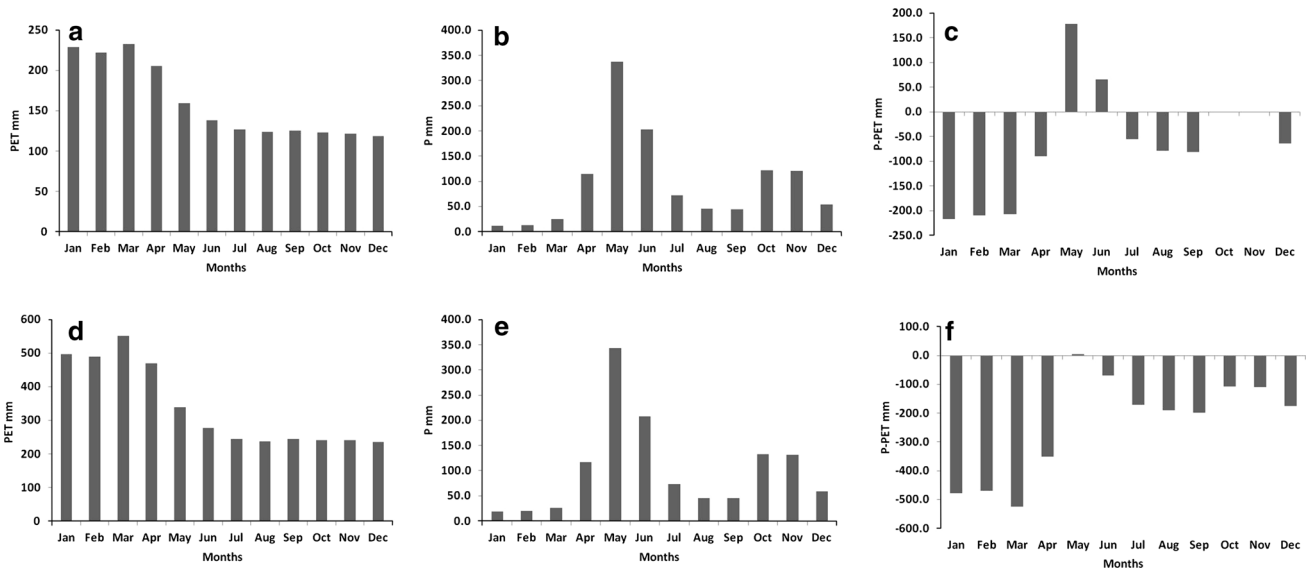

Fig. 8 Graphs showing the predicated average monthly potential precipitation (PET) (**a**, **d**) and precipitation (P) (**b**, **e**) as well as P–PET (**c**, **f**) for 2090s for A1b and A2 SRES

$$S_a = S_h + S_z = (1+G)\frac{\pi a^2}{4}\sqrt{\frac{w}{K(1+G)}}. \quad (4)$$

Note that the value of a is the average length of two successive profile lines.

The water volume in each transect was obtained by multiplying the surface S_a of each profile with the distance in between them, 500 m, and the porosity, φ. The total volume, V, was obtained by adding up the volumes of all 23 slices. The porosity, φ, of the aquifer is 30 % (Kuria 2008).

$$V = 500 S_a \varphi \quad (5)$$

Drawdown and up-coning due to pumping wells

To calculate the drawdown of a single partial penetrating pumping well of a known depth, the Neuman solution (1975) was used.

$$h_0 - h = \frac{Q}{4\pi T} W(U_B, \Gamma) \quad (6)$$

where $W(U_B,\Gamma)$ is the well function for the water table aquifer, as tabulated by Neuman (1975) and adapted by (Fetter 2001)

$$U_B = \frac{r^2 S_y}{4Tt} \text{ (for steady} - \text{state drawdown)} \quad (7)$$

$$\Gamma = \frac{r^2 K_v}{b^2 K_h} \quad (8)$$

where h_0-h_f is the drawdown (L; m), Q is the pumping rate (L^3/T; m^3/d), T is the transmissivity (L^2/T; m^2/d), r (L; m), S_y is the specific yield (dimensionless), t is the time (T; d), K_h and K_v are the horizontal and vertical hydraulic conductivity (L/T; m/d), b is the initial saturated thickness of the aquifer (L; m) (as shown in Fig. 7).

The term u represents the up-coning (the movement of saltwater from a deeper saltwater zone upward into the fresh groundwater in response to pumping at a single well) and was calculated by applying the Ghyben–Herzberg relationship from Eq. (3) to the top of the water table height, h_0-h_f, derived from Eq. (6).

$$u = 31.25(h_0 - h_f) \quad (9)$$

It should be noted that the Ghyben–Herzberg relationship is used with the Dupuit assumption that the only horizontal flow was relevant in the profile (Haubold 1975). The other assumptions made for this model used are that Darcy's law is valid, the aquifer is unconfined, the vadose zone has no influence on the drawdown, all flows towards the well are radial and the aquifer may be—but does not have to be—anisotropic (Fetter 2001).

The volume of the drawdown V_d and up-welling V_u cones was calculated using the equation for a cone and multiplied by the porosity

$$V_d = \frac{1}{3}\pi r^2 (h_0 - h_f)\varphi \quad (10)$$

$$V_u = \frac{1}{3}\pi r^2 u \varphi \quad (11)$$

V_d is the total volume of the freshwater p whereas V_u is the volume of freshwater in the aquifer lost to salinization as a result of the well pumping.

The total volume of drawdown and up-welling, i.e. $V_d + V_u$ is the amount of freshwater lost from the freshwater lens from a single well. As the study area has 30 wells and we assume the same pumping rate on each one of them, the total volume of freshwater lost, V_s, is obtained from

$$V_s = 30(V_d + V_u) \quad (12)$$

Effective freshwater volume

The effective volume of the freshwater lens was calculated by subtracting the sum of the volume of the drawdown and up-welling V_s (Eq. 9) from the total volume, V (Eq. 5).

$$V_a = V - V_s \quad (13)$$

Size reduction of the freshwater lens under the influence of climate change

Seasonal predictions of changes in temperature and precipitation for the 2090s (10-year time series between 2090 and 2100) for both A1b and A2 SRES' were obtained from those outlined in McSweeney et al. (2010a). Monthly changes were calculated from McSweeney et al. (2010a) seasonal predictions. The statistical downscaling methodology used on the global climate models to obtain values for Kenya is described in McSweeney et al. (2010b, c). Climate data provided by KMD were used to calculate a monthly average for ten-year average (2001–2011). The present-day climate data were grouped into seasons for compliance with the future predictions and the percentage seasonal variation calculated. These percentages were then applied to the individual months to get the expected monthly change (Tables 1, 2).

The Thornthwaite (1948) method was used to estimate future PET (PET_1') for the 2090s in the A1b and A2 SRES (Intergovernmental Panel on Climate Change (IPCC 2007). Thornthwaite's equation calculates monthly values of PET_1' (in mm) based on a standard month of 30 days and 9 h of sunlight/day (average for Lamu) and is expressed as

$$PET_1' = C\left(\frac{T_a}{l}\right)^a \quad (14)$$

where $C = 16$ is a constant and $a = 67.5 \times 10^{-8} I^3 - 77.1 \times 10^{-6} I^2 + 0.0179 I + 0.492$.

The annual value of the heat index I is calculated by summing monthly indices over a 12-month period. The monthly indices are obtained from the equations

$$i = \left(\frac{T_a}{5}\right)^{1.51} \quad (15)$$

and

$$l = \sum_{j=1}^{12} i_j \quad (16)$$

Table 1 Expected monthly increases in temperature using predicted seasonal changes and current climate data

Month	Observed mean temp. 2001–2011	Predicted monthly A1b	Predicted monthly A2
Jan	28.5	31.6	25.1
Feb	28.6	31.7	25.2
Mar	29.7	25.7	33.6
Apr	29.5	25.6	33.4
May	28.0	30.9	31.7
Jun	26.7	29.9	30.6
Jul	26.1	29.3	29.9
Aug	26.1	29.3	30.0
Sep	26.8	30	30.7
Oct	27.6	30.2	31.0
Nov	28.1	30.8	31.5
Dec	28.4	31.1	31.8

Table 2 Expected monthly increases in rainfall using predicted seasonal changes and current climate data

Month	Observed mean rainfall 2001–2011	Predicted monthly A1b	Predicted monthly A2
Jan	1.7	11.7	18.7
Feb	1.8	12.4	19.8
Mar	23.6	25.5	26.0
Apr	106.4	115.1	117.3
May	311.2	336.7	342.9
Jun	201.0	203.2	207.6
Jul	71.2	72	73.5
Aug	44.1	45.1	45.6
Sep	43.6	44.1	45.0
Oct	96.4	124.2	125.1
Nov	95.6	121.2	131.0
Dec	42.9	54.4	58.8

where I is the annual heat index, i is the monthly heat index for the month j (which is zero when the mean monthly temperature is 0 °C or less), Ta is the mean monthly air temperature (°C), and j is the number of months (1–12).

The monthly PET_1' were adjusted depending on the number of days, N, in a month ($1 \leq N \leq 31$) and the duration of the average monthly or daily daylight d (in hours), which is a function of season and latitude.

$$PET_1 = PET_1'\left(\frac{d}{12}\right)\left(\frac{N}{30}\right) \quad (17)$$

where PET_1 (and PET_2) is the adjusted monthly PET (mm), d is the duration of average monthly daylight (taken to be 9 h), and N is the number of days in a given month, 1–31

(days). The formulas used are Xu and Singh (2001) adaptation of the Thornthwaite (1948) equation.

Future potential recharge was calculated by subtracting PET_1 from the precipitation P_1 (for A1b) and PET_2 from the precipitation P_2 (for A2). The months with a P–PET value larger than zero (May and June for A1b and none for A2 as seen in Fig. 8) were considered to be the months where recharge of the aquifer would occur giving the total annual recharge. The daily potential recharge was derived by dividing this annual recharge by number of days in a year, i.e. 365.

The effect of climate change on the saltwater density as a result of changes in temperature and salinity as suggested by Uddameri et al. (2014) was modelled. The salinities of the saltwater under A1b and A2 scenarios were obtained using the Lewis and Parkins (1981) conversion calculator taking into consideration the projected temperature changes. The new salinities were used to calculate new G values for the SRES (Indian Ocean's conductivity in Lamu was recorded at 49.2 ms).

These new recharge data and G values were used in Eq. (4) to calculate the new cross-sectional areas of the profiles and Eq. (5) and the total freshwater volumes in the aquifer respectively for both A1b and A2 scenarios.

Saltwater intrusion indicator

Salinization of the groundwater due to saltwater intrusion in the Shela aquifer was characterized using the vulnerability indicator M presented by Werner et al. (2012). The M indicator is a mixed convection ratio defined as:

$$M = \frac{K\delta(1+\delta)\xi^2}{wx_n^2} \tag{18}$$

where x_n is the inland distance of the no flow boundary, ξ is the thickness of the unconfined aquifer (in this case the average thickness was used), and δ is a dimensionless density term defined as

$$\delta = \frac{\rho_s - \rho_f}{\rho_f} \tag{19}$$

The M saltwater intrusion indicator used in this study was modified by Antonellini et al. (2014) to accommodate for changes in recharge and sea level rise due to climate change by introducing the α ratio between the net recharge of the aquifer for 2090s (w_{2090s}) and the net recharge of the aquifer for year 2001–2011 ($w_{2001-2011}$).

The increase in sea level due to climate change Δz (m) for the end of the century was derived from global mean sea level predictions of 0.43 m for A1b (Kebede et al. 2010) and 0.48 m for A2 scenarios (Johns et al. 2003; Carneiro et al. 2010). It was applied in the Eq. (20) to derive the parameter β by increasing the thickness of the aquifer at the coastline as suggested by Werner and Simmons (2009)

$$\beta = \left(1 + \frac{\Delta z}{z}\right) \tag{20}$$

To accommodate the effects of a change in sea level and in recharge driven by climate change, following Antonellini et al. (2014), the M parameter can be re-written to M_{cc} as

$$M_{cc} = \frac{K\delta(1+\delta)\beta^2\xi^2}{\alpha w x_n^2} \tag{21}$$

It is reasonable to assume that parameters such as K, δ, and x_n do not vary much as a result of climate change, so M_{cc} will be re-written as

$$M_{cc} = \frac{\beta^2}{\alpha} M \tag{22}$$

which is the relative vulnerability of the aquifer under the influence of climate change driven by sea level rise and recharge.

Results and discussion

Freshwater lens size and shape

The potential recharge, w, using LocClim has been estimated to be 2.82E−4 m/d whilst the water table at the well in plot line 10 has been found to be 1.7 m. These values were used in Fetter's Infinite-Strip Island to calculate the hydraulic conductivity, K, of the Shela aquifer, which has been estimated to be 0.755 m/d.

The highest point of elevation of the water table of the test profile (10) has been estimated to be 1.7 m.a.s.l., which coincided with well depth and water column data provided by Kuria (2008) and sand dune elevation data acquired using GIS and DEMs. As per the DEMs, the elevation above sea level at the centre of the profile 10, which is also the exact location of well 30 in the Shela well field, is 17 m.a.s.l. According to Kuria (2008), the well is 14.8 m deep with a 0.5-m water column, giving a water table elevation of 1.7 m. The water table elevation along the entire length of the dunes varies from 1.2 to 4 m.a.s.l., with an average height of 2 m.a.s.l. The highest water table levels (2.5–4 m.a.s.l.) are in west of the sand dunes in the Kizunguni/Kipungani area, where the dunes reach heights of 65 m. The lowest levels are in the east in the area underlying the Shela well field and range from 1.2 to 1.6 m.a.s.l. (Fig. 9a). Water withdrawal, which has been going on since the 1950s, combined with altered topography of the sand dunes due to human settlement is a possible

cause for the lower water table of this area in comparison to the western area. The Kizunguni/Kipungani area has a lower occurrence of human settlements and a lower population density resulting in the dunes maintaining their relatively pristine conditions. The Shela area, on the other hand, has a high level of human interference. Aside from the wells and the Shela pump house constructed a short distance away, there are access roads over and between the dunes that have negatively impacted them resulting in lower dunes elevation of as low as 8 m.a.s.l. and consequently affecting the water table level.

The computed depth of the interface below sea level ranges from −40 m.a.s.l. in the east to −160 m.a.s.l. in the west. The average depth of the freshwater lens is −80 m.a.s.l. According to the results of this study, the lowest value ξ for the freshwater lens thickness (shallowest part) of the aquifer is in the area below the Shela well fields whereas the area with the highest ξ is to the west, furthest away from the wells (Fig. 9b). Kuria (2008) made geo-electrical surveys in the Shela aquifer along nine tomography lines within the sand dunes. In his geo-electrical resistivity models along these tomography lines, the depth of the freshwater lens below the dunes was detected. Similarities in freshwater depth between the tomography lines and the depths of this study are evident. For example, a tomography line that lies between profiles 4 and 5 of this study has a freshwater lens extending beyond a depth of −131 m.a.s.l. It lies between two profiles that have depths of −150 and −125 m.a.s.l., respectively. Conversely, tomography line 5 that lies between this study's profiles 12 and 13 shows two areas of low resistivity at the top of tomography line, which correspond with the locations of the wells. Below tomography line 5, at a depth of −43 m.a.s.l. extending downwards to −131 m.a.s.l., an area of low resistivity indicates possible up-coning of salt water.

From monthly water withdrawals data derived from LAWASCO, it was established that 49 m^3 of water was pumped per day per well. The size and volume of the drawdown cone below each well in steady-state conditions were calculated using the Neuman solution and the related up-coning from the Ghijben-Herzberg relationship (Bear 1972). The average maximum depth of the drawdown cone has been determined as −1.69 m.a.s.l. below the water table which results in a maximum up-coning of 52 m (maximum height at the centre of the cone). The saltwater up-coning resulting from point abstraction in the Shela well field is one possible explanation for the comparatively shallow freshwater/saltwater interface under the well fields as observed by the different freshwater lens thickness results for the east and the west of the aquifer (Table 3). Based on the analytical computations performed in this work, the average depth of the interface below the wells is −54 m.a.s.l., 26 m shallower than the average depth below the entire dune system that is −80 m.a.s.l. Further east, away from the well fields close to the Shela settlement, the interface deepens further to −59 m.a.s.l. With 30 wells in the field close together [at least 20 wells are fully operational according to Kuria (2008)], the rate of up-coning is bound to be high as well as the added possibility of up-

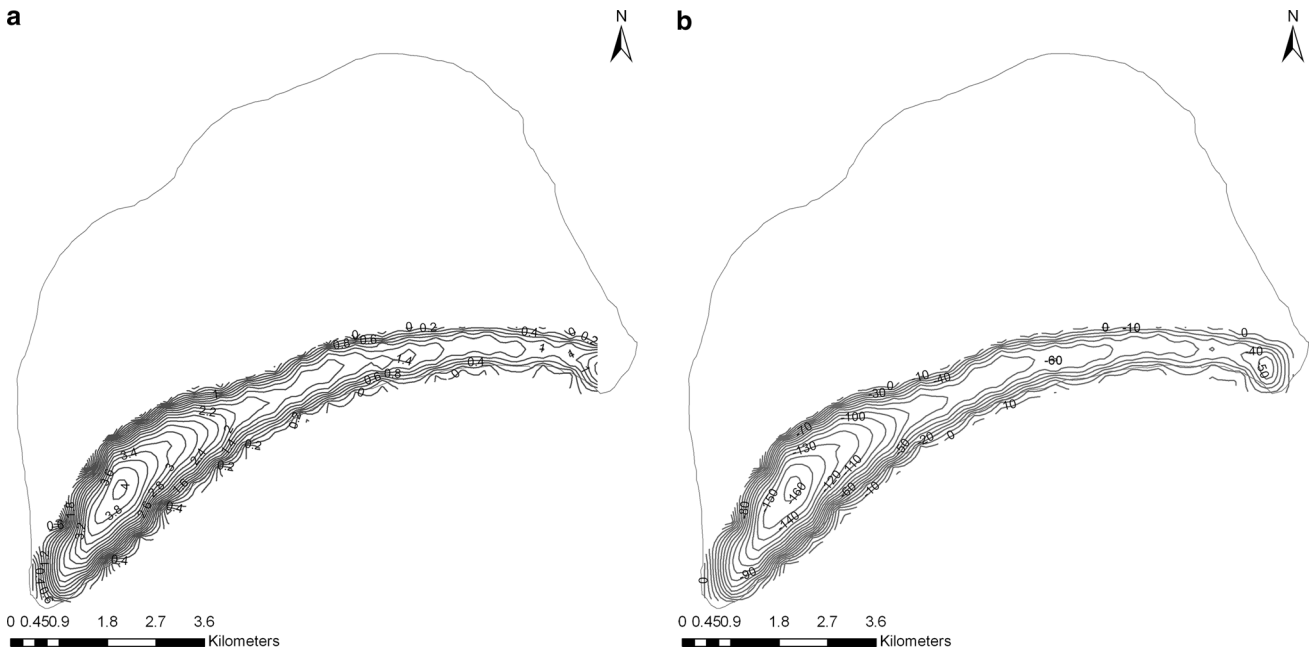

Fig. 9 Contour maps of the Shela aquifer showing (**a**) water table elevation above sea level and (**b**) freshwater/saltwater interface depths

Table 3 Summary of the results of Fetter's Infinite-Strip Island for K and h_f for all profile lines as well as area and volume calculations

Profile	w (mm)	G	K (m/d)	R (m)	r (m)	h_f (m.a.s.l)	ξ (m.a.s.l)	A (m^2)	Volume (m^3)
1	0.0002816	31.25	0.755	892.5	100	2.47	98.62	68563.78	34281889.18
2	0.0002816	31.25	0.755	1116.5	100	3.6	144.19	107,299.02	53649509.03
3	0.0002816	31.25	0.755	1,141.5	100	3.99	159.56	112,157.97	56,078,982.96
4	0.0002816	31.25	0.755	1,042	100	3.77	150.99	93,457.41	46,728,703.87
5	0.0002816	31.25	0.755	908.5	100	3.31	132.49	71,044.12	35,522,061.38
6	0.0002816	31.25	0.755	766.5	100	2.87	114.67	50,571.12	25,285,562.27
7	0.0002816	31.25	0.755	630	100	2.35	93.86	34,163.27	17,081,633.36
8	0.0002816	31.25	0.755	545	100	1.94	77.54	25,566.50	12,783,250.57
9	0.0002816	31.25	0.755	510	100	1.77	70.73	22,388.17	11,194,086.26
10	0.0002816	31.25	0.755	500	100	1.7	68.01	21,518.81	10,759,406.25
11	0.0002816	31.25	0.755	480	100	1.7	68.01	19,831.74	9,915,868.80
12	0.0002816	31.25	0.755	452	100	1.56	62.57	17,585.52	8,792,758.94
13	0.0002816	31.25	0.755	438.5	100	1.51	60.4	16,550.74	8,275,371.37
14	0.0002816	31.25	0.755	413	100	1.47	58.9	14,681.77	7,340,884.66
15	0.0002816	31.25	0.755	373.5	100	1.34	53.46	12,007.69	6,003,845.52
16	0.0002816	31.25	0.755	354.5	100	1.2	48.15	10,817.10	5,408,549.09
17	0.0002816	31.25	0.755	348.5	100	1.2	48.29	10,454.03	5,227,016.39
18	0.0002816	31.25	0.755	322	100	1.16	46.52	8,924.63	4462313.11
19	0.0,002,816	31.25	0.755	299	100	1.03	41.08	7,695.21	3,847,606.71
20	0.0002816	31.25	0.755	364.5	100	1.01	40.26	11,435.98	5,717,989.62
21	0.0002816	31.25	0.755	433	100	1.14	58.9	16,138.16	8,069,081.27
East	0.0002816	31.25	0.755	362.5	100	1.23	49.31	11,310.83	5,655,412.91
West	0.0002816	31.25	0.755	216.5	100	0.73	29.44	4,034.54	2,017,270.32
								V	128,033,017.95
								V_s	4,342,442.29
								V_a	123,690,575.66

cones overlapping, which would cause a cumulative rise of the freshwater/saltwater interface.

The results show that the total volume lost for all 30 wells is 0.2×10^6 m^3 drawdown and 4.1×10^6 m^3 from saltwater up-coning, adding up to a total of $\approx 4.3 \times 10^6$ m^3 lost annually from abstraction for human consumption and the resultant infiltration of salt or brackish water into the freshwater lens. To determine the effective volume of the freshwater lens, these losses were subtracted from the total saturated volume of the freshwater aquifer (Table 3). The total saturated volume of the freshwater lens is 128×10^6 m^3 whereas the volume after discharge and saltwater up-coning had been taken into account is estimated to be approximately 124×10^6 m^3. This represents a 3.4 % loss of freshwater caused directly or indirectly by human abstraction.

Impacts of climate change on recharge

According to Findlay (2003), water availability will be limited in many regions of the world by climate change. One of the most severe consequences of climate change will be the alteration of the hydrological cycle, which will impact on the quantity and quality of regional water resources (Gleick and Adams 2000). Changes in temperature and precipitation affect groundwater recharge and cause shifts in water tables and consequently changes in their volumes as a first response to climate change (Changnon et al. 1988; Zektser and Loaiciga 1993; Ali et al. 2012b). This may result in problems with future water supply for large sections of the world population living in the coastal zones (Ramon Raposo et al. 2013). According to McSweeney et al. (2010a), the future average increase in temperature is expected to range from 3 °C to 3.7 °C for A1b and A2 SRES, respectively (representing a 10.7 and 13.2 % increase from the current average) These temperatures would result in the saltwater density increasing to 1.0302 g/cm^3 for A1b and 1.0298 g/cm^3. The precipitation is projected to increase by 11–16 mm a year reflecting a 156.1 and 262.6 % increment for the same SRES from the current average. Using Thornwaite's equation to compute PET, the potential recharge for the A1b SRES has been computed to be 0.66 mm/d and 0.0134 mm/d, representing an increase of 0.38 mm/d (135 %) for A1b and 2.7 mm/d

(81 %) decrease for A2 from the current average (Tables 1, 2).

Groundwater in shallow aquifers is affected by changes in the hydrologic cycle and by climate variability and change through recharge processes (Chen et al. 2002). Consequently, climate change affects the availability of freshwater for both ecosystem and human uses (Carpenter et al. 1992; IPCC 2001; Ramon Raposo et al. 2013). This change in recharge will have an impact on the size of the freshwater lens. Under A1b conditions, G is expected to increase to 33.11 resulting in an increase in the volume of the water in the aquifer 199×10^6 m^3. In contrast, a reduced recharge for the A2 scenario, where G increases to 33.56, resulting in a decrease in volume to 27×10^6 m^3 is projected. The results of the A2 scenario are in line with many climate change studies that predict reduced recharge (Serrat-Capdevila et al. 2007; Wegehenkel and Kersebaum 2009; Ali et al. 2012a). The effects of climate change on recharge, however, may not necessarily be negative in all aquifers (Green et al. 2011) as demonstrated by Stoll et al. (2011) in a catchment in northern Switzerland. The results showing an increase in recharge for the A1b scenario and consequently the volume of the freshwater lens in this study presents further evidence for this possibility.

Vulnerability assessment

Saltwater intrusion in coastal aquifers will be exacerbated by sea level rise and climate change. It is therefore important to assess the vulnerability of the Shela aquifer to this intrusion considering different climate change scenarios. A useful methodology developed by Werner et al. (2012) method is an approach used to quantify how much surface of the coastal zone is invaded by saltwater as a result of sea level rise and potential recharge. Werner et al. (2012) develop the M mixed convection ratio that could be used as a saltwater intrusion indicator ($M = 1$ worst-case scenario with extensive saltwater intrusion; $M = 0$ best scenario with no saltwater intrusion). Here, the analysis of the M indicator was used to show how it will change in the future relatively to today's condition (M today $= M-$ which was found to be 0.04). When future recharge and sea level rise are taken into consideration for the A1b scenario, the M_{cc1} value was found to be 0.5 M translating to a reduction in the vulnerability from the present situation by a factor of 0.5 (decrease by half) primarily because of increased potential recharge. This suggests that despite the expected increase in temperature, the increase in rainfall will result in higher recharge with respect to present conditions. This increase in volume of the freshwater lens and lower vulnerability will be beneficial to the local population and ecosystems supported by the aquifer. Conversely, the vulnerability of the aquifer to saltwater intrusion (M_{cc2}) in the A2 scenario increases greatly by a factor of 24.9 in relation to M (24.9 M) primarily because of the increased PET. In spite of the increase in rainfall projected for this scenario, the great increase in temperature is expected to negatively impact the potential recharge.

The results of this vulnerability assessment are useful for freshwater management policies in Kenya where at least 24 % of the population do not have access to clean, safe drinking water (Leiter et al. 2013). This integrated water resource management needs to consider all water issues and management options as well as meet international development goals. They also have to include challenges from the accelerating global and regional climate change and the morphing society (Schanze et al. 2012). The draft National Water Policy (NWP) (Republic of Kenya 2012b) highlights that groundwater assessment, research and development, monitoring, and controlling of groundwater exploitation in Kenya shall take into consideration the potential groundwater resources and the need for sustainable use. For this to be successful, proper data collection, analysis, and interpretation for adequate regulation are required. Particular attention should be paid on controlling non-intrusion of saltwater into freshwater aquifers, taking actions on overexploitation of aquifers, whilst exploring virgin and unexploited aquifers. The results of the vulnerability assessment not only fill in the information gap by providing empirical data, but also highlight the Shela aquifer's risk level and susceptibility to salinization. This will be important information to be taken into consideration as the construction of the new port continues.

As discussed earlier, the up-coning is a direct impact of abstraction for human use. The freshwater/saltwater interface below the well fields is considerably shallower as a result of this saltwater encroachment. With the construction of a new port in Lamu already underway, the population on the Lamu Island dependent on the Shela aquifer for freshwater is set to increase from 22,000 as at present to 1.25 million people by 2050 (Republic of Kenya 2011). Continued reliance on groundwater sources like the Shela aquifer with over 5500 % population growth expected will further compound the effects climate change will have on saltwater intrusion. If a linear increase in withdrawal of water from the aquifer to meet the increasing demand driven by population increase is to be assumed, the freshwater bubble is expected to be exhausted by 2033 and fail as a source of water. The discovery of new sources of freshwater to support the extreme population growth brought about by the new metropolis is therefore a necessity and must to be taken into consideration as the construction of the new infrastructure proceeds. This is the basis of a follow-up study (Okello et al. in preparation). So far, the Environmental and Social Impacts Assessment (Republic of Kenya 2013) studies carried out in the area in

regard to water management concentrate on the water quality of the Indian Ocean surrounding east of Manda Island (Fig. 1). Neither provision of freshwater nor vulnerability to saltwater intrusion has not been considered by these studies.

Conclusions and recommendations

With limited data about Lamu Island in general and the Shela aquifer in particular, this study has demonstrated that analytical solutions can be used to calculate the size and shape of the freshwater lens, the location of the freshwater/saltwater interface as well as the hydraulic conductivity in an aquifer where very limited hydrogeological information is available. Quantification and characterization of the aquifer and the effect of climate change under SRES scenarios A1b and A2 at the end of this century on freshwater resources have been established. The water table elevation at various points of the aquifer (ranging 1.2–4 m.a.s.l.) has been established with different methodologies such as Fetter's Infinite Island Strip and using DEMS and ArcGIS. From these elevations, the corresponding depth of the freshwater/saltwater interface at these points was also calculated. The total saturated volume of the freshwater lens before abstraction (128×10^6 m^3) and the effective volume after discharge and saltwater intrusion (124×10^6 m^3) were approximated, representing 3.4 % loss in volume to human abstraction. Future climate change scenarios have also been modelled and show that under the A1b SRES, a 136 % increase of recharge is expected and an increase in the effective freshwater volume to 199×10^6 m^3. The aquifer's vulnerability is expected to reduce by half (50 %) from the current state under these climatic conditions. This is a sharp contrast to the A2 scenario where an opposite impact is expected. The recharge in A2 is expected to decrease by 95 % and the effective volume is expected to reduce to 27×10^6 m^3. The aquifer is expected to be more vulnerable to saltwater intrusion under these conditions with the M value increasing by a factor of 24.9.

This study provides sound methods of data collection, analysis, and interpretation needed by policy makers in regard to groundwater assessment, research and development, monitoring, and controlling of groundwater exploitation globally. For the results to be fortified, a test pumping program should be carried out on all the wells using piezometric wells to establish their safe yields. This will contribute in the alleviation of saltwater intrusion issue by managing the amount of water drawn from each well. Furthermore, a monitoring program of the water quantity and quality in the well field should be established. Water management policies of the Kenyan coast generally and the Lamu area specifically should take into account the effect the new harbour will have on population growth and land-use changes. Considering that industrialized agriculture contributes to climate change and biodiversity decline, this policy should ensure that coastal groundwater resources with their associated ecosystems are safeguarded. This can be done by ensuring that the freshwater/saltwater balance is maintained. A vulnerability indicator that combines the effects of climate change, sea level rise and the anthropogenic contribution would give a better risk assessment to saltwater intrusion, providing policymakers a clearer analysis of the situation.

Acknowledgments This research was carried out as part of the Erasmus Mundus Joint Doctorate Program in Marine and Coastal Management primarily in the University of Bologna's Ravenna campus in the Integrated Geoscience Research Group (I.G.R.G.) which part of Interdepartmental Centre for Environmental Sciences Research (CIRSA). Thank you to all my colleagues for the support they have given me throughout the research period. A special mention is reserved for University of Cadiz for the coordination/administration of the program.

References

Ali R, Mcfarlane D, Varma S, Dawes W, Emelyanova I, Hodgson G (2012a) Potential climate change impacts on the water balance of regional unconfined aquifer systems in south-western Australia. Hydrol Earth Syst Sci 16:4581–4601. doi:10.5194/hess-16-4581-2012

Ali R, Mcfarlane D, Varma S, Dawes W, Emelyanova I, Hodgson G, Charles S (2012b) Potential climate change impacts on groundwater resources of south-western Australia. J Hydrol 475:456–472

Anderson WP Jr, Evans DG, Snyder SW (2000) The effects of Holocene barrier island evolution on water-table elevation, Hatteras Island, North Carolina, USA. Hydrogeol J 8:390–404

Antonellini M, Dentinho T, Khattabi A, Masson E, Mollema PN, Silva V, Silveira P (2014) An integrated methodology to assess future water resources under land use and climate change: an application to the Tahadart drainage basin (Morocco). Environ Earth Sci 71:1839–1853. doi:10.1007/s12665-013-2587-5

Archer DC (2012) Energy system assessment and modeling of a potential future energy system on Lamu Island, Kenya A case study relevant for many regions with similar climatic conditions, Master thesis within the Sustainable Energy Systems program, Department of Energy and Environment Division of Energy Technology, Chalmers University of Technology

Badon Ghijben W (1888) Nota in verband met de voorgenomen putboring nabij Amsterdam [Notes on the probable results of a well drilling near Amsterdam]. Tijdschrift Koninklijk Instit Ing (1988/1989), pp 8–22

Barlow PM (2003) Groundwater in freshwater–saltwater environments of the Atlantic Coast. US Geol Surv Circ 1262, p 121

Barlow PM, Reichard EG (2010) Saltwater intrusion in coastal regions of North America. Hydrogeol J 18:247–260. doi:10.1007/s10040-009-0514-3

Bear J (1972) Dynamics of fluids in porous media. Dover Publications, USA

Bear J, Cheng AHD, Sorek S, Ouazar D, Herrera I (eds) (1999) Seawater intrusion in coastal aquifers-concepts, methods and practices. Kluver Academic Publishers pp 163–191

Beyer WH (2013) C.R.C. Standard mathematical tables, 24th edn., CRC Press

Bobba AG, Singh VP, Berndtsson R, Bengtsson L (2000) Numerical simulation of saltwater intrusion into Laccadive island aquifers due to climate change. J Geol Soc India 55:589–612

Brown S, Kebede AS, Nicholls RJ (2009) Sea-Level Rise and impacts in Africa, 2000 to 2100. University of Southampton, Southampton, UK, Unpublished Report to Stockholm Environment Institute, p 215

Budd DA, Vacher HL (1991) Predicting the thickness of fresh-water lenses in carbonate paleo-islands. J Sediment Petrol 61:43–53

Carneiro JF, Boughriba M, Correia A, Zarhloule Y, Rimi A, El Houadi B (2010) Evaluation of climate change effects in a coastal aquifer in Morocco using a density-dependent numerical model. Environ Earth Sci 61:241–252

Carpenter S, Fisher S, Grimm N, Kitchell JF (1992) Global change and freshwater ecosystems. Ann Rev Ecolog Syst 23:119–137

Cartwright N, Li L, Nielsen P (2004) Response of the salt–freshwater interface in a coastal aquifer to a wave-induced groundwater pulse: field observations and modelling. Adv Water Resour 27:297–303

Changnon SA, Huff FA, Hsu CF (1988) Relations between precipitation and shallow groundwater in Illinois. J Clim 1:1239–1250

Chen ZH, Grasby SE, Osadetz KG (2002) Predicting average annual groundwater levels from climatic variables: an empirical model. J Hydrol 260:102–117

Collins WH, Easley DH (1999) Fresh-water lens formation in an unconfined barrier-island aquifer. J Am Water Resour Assoc 35:1–21

Custodio E (2010) Coastal aquifers of Europe: an overview. Hydrogeol J 18:269–280. doi:10.1007/s10040-009-0496-1

Desanker P, Magadza C, Allali A et al (2001) In: McCarthy JJ, Canziani OF, Leary NA, Dokken DJ, White KS (eds) Climate Change: Impacts, Adaptation, and Vulnerability. Cambridge University Press, Cambridge, UK, p 1032

Essink G (2001) Improving fresh groundwater supply—problems and solutions. Contribution of working group II to the third assessment report of the intergovernmental panel on climate change. Ocean Coast Manag 44:429–449

Essink G, van Baaren ES, de Louw PGB (2010) Effects of climate change on coastal groundwater systems: a modeling study in the Netherlands. Water Resour Res 46:W00F04. doi:10.1029/2009WR008719

FAO (2002) LocClim Local climate estimator. A computer application developed by Juergen Grieser based on FAOCLIM ver. 2 database of the Agrometeorology Group, FAO Environment and Natural Resources Service SDRN. SDRN Working Paper Series Publ. no. 9, FAO, Rome

Fetter CW (1972) Position Of Saline Water Interface Beneath Oceanic Islands. Water Resour Res 8:1307

Fetter CW (2001) Applied Hydrogeology, 4th edn. Prentice Hall Inc., New Jersey, p 598

Findlay R (2003) Global climate change: implications for water quality and quantity. J Am Water Works Assoc 95:36

Giupponi C, Mordechai S (2003) Climate Change in the Mediterranean. Edward Elgar Publishing, Northampton

Gleick PH, Adams DB (2000) The potential consequences of climate variability and change of the water resources of United States. A special report for the US Global Research Program. US Geol Survey

Green TR, Taniguchi M, Kooi H, Gurdak JJ, Allen DM, Hiscock KM, Treidel H, Aureli A (2011) Beneath the surface of global change: impacts of climate change on groundwater. J Hydrol 405:532–560

Harris WH (1967) Stratification of fresh and salt water on barrier islands as a result of differences in sediment permeability. Water Resour Res 3(1):89–97

Haubold RG (1975) Approximation for steady interface beneath a well pumping fresh water overlying salt water. Ground Water 13:254–259

Herzberg A (1901) Die Wasserversorgung einiger Nordseebaeder [The water supply of selected North Sea towns]. Z F Gasbeleucht Wasserversorg 44:815–844

Intergovernmental Panel on Climate Change (IPCC) (2000) IPCC Special report emissions scenarios: summary for decision makers. IPCC, Italy

Intergovernmental Panel on Climate Change (IPCC) (2001) Climate Change 2001: impacts, adaptation, and vulnerability. Contribution of Working Group II to the Third Assessment Report of the Intergovernmental Panel on Climate Change. Cambridge University Press, Cambridge

Intergovernmental Panel on Climate Change (IPCC) (2007) Summary Policymakers. In: Solomon S, Qin D, Manning M, Chen Z, Marquis M, Averyt KB, Tignor M, Miller HL (eds) Climate change 2007: the physical science basis.Contribution of Working Group I to the Fourth Assessment Report of the Intergovernmental Panel on Climate Change. Cambridge University Press, Cambridge, p 18

Johns TC, Gregory JM, Ingram WJ et al (2003) Anthropogenic climate change for 1860 to 2100 simulated with the HadCM3 model under updated emissions scenarios. Clim Dyn 20:583–612

Kattaa B, Al-Fares W, Al Charideh AR (2010) Groundwater vulnerability assessment for the Banyas Catchment of the Syrian coastal area using GIS and the RISKE method. J Environ Manage 91:1103–1110

Kebede AS, Nicholls RJ, Hanson S, Mokrech M (2010) Impacts of climate change and sea-level rise: a preliminary case study of Mombasa, Kenya. Tyndall Centre for Climate Change Research Working Paper 146

Kuria ZN (2008) A scientific assessment of the groundwater (aquifers) along the gazetted Shella water catchment area, Lamu Island. Final report prepared for the National Museums of Kenya

Langevin CD, Swain ED, Wolfert MA (2005) Simulation of integrated surface-water/ground-water flow and salinity for acoastal wetland and adjacent estuary. J Hydrol 314(1–4): 212–234

Leiter M, Levy J, Mutiti S, Boardman M, Wojnar A, Deka H (2013) Drinking water quality in the Mount Kasigau region of Kenya: a source to point-of-use assessment. Environ Earth Sci 68:1–12. doi:10.1007/s12665-012-1698-8

Lobo Ferreira JP, Chachadi AG, Diamantino C, Henriques MJ (2007) Assessing aquifer vulnerability to seawater intrusion using the GALDIT method: part 1 Application to the Portuguese Monte Gordo aquifer. Water in Celtic Countries: quantity, quality and climate variability 310: 161–171

Maas K (2007) Influence of climate change on a Ghijben-Herzberg lens. J Hydrol 347:223–228. doi:10.1016/j.jhydrol.2007.09.020

McSweeney C, New M, Lizcano G (2010a) UNDP climate change country profiles: Kenya. http://country-profiles.geog.ox.ac.uk. Accessed June 19, 2014

McSweeney C, New M, Lizcano G (2010b) UNDP climate change country profiles: Documentation. http://country-profiles.geog.ox.ac.uk. Accessed June 19, 2014

McSweeney C, New M, Lizcano G (2010c) The UNDP climate change country profiles: improving the accessibility of observed and projected climate information for studies of climate change in developing countries. Bull Am Meteorol Soc 91:157–166

Mollema PN, Antonellini M (2013) Seasonal variation in natural recharge of coastal aquifers. Hydrogeol J 21:787–797. doi:10.1007/s10040-013-0960-9

Mollema PN, Antonellini M, Dinelli E, Gabbianelli G, Greggio N, Stuyfzand PJ (2013a) Hydrochemical and physical processes influencing salinization and freshening in Mediterranean low-lying coastal environments. Appl Geochem 34:207–221

Mollema PN, Antonellini M, Gabbianelli G, Galloni E (2013b) Water budget management of a coastal pine forest in a Mediterranean catchment (Marina Romea, Ravenna, Italy). Environ Earth Sci 68:1707–1721

Neuman SP (1975) Analysis of pumping test data from anisotropic unconfined aquifers considering delayed gravity response. Water Resour Res 11:259–342

Nyenje PM, Batelaan O (2009) Estimating the effects of climate change on groundwater recharge and baseflow in the upper Ssezibwa catchment, Uganda. Hydrological Sciences Journal–Journal Des Sciences Hydrologiques 54:713–726

Peng L, Zhanbin L, Kexin L (2004) Effect of vegetation cover types on soil infiltration under simulating rainfall. 13th International Soil Conservation Organisation Conference

Ramon Raposo J, Dafonte J, Molinero J (2013) Assessing the impact of future climate change on groundwater recharge in Galicia-Costa, Spain. Hydrogeol J 21:459–479

Ranjan SP, Kazama S, Sawamoto M (2006) Effects of climate and land use changes on groundwater resources in coastal aquifers. J Environ Manage 80:25–35

Ranjan P, Kazama S, Sawamoto M, Sana A (2009) Global scale evaluation of coastal fresh groundwater resources. Ocean Coast Manag 52:197–206

Reilly TE, Goodman AS (1987) Analysis of saltwater upconing beneath a pumping well. J Hydrol 89:169–204

Republic of Kenya (1991) Groundwater resources assessment of Lamu island and the Hindu-Mokowe area, Lamu district. Ministry of Reclamation and Development of Arid, Semi-arid areas and Wasterlands, Coastal ASAL Development Project

Republic of Kenya (2011) LAPSSET corridor and new Lamu port feasibility study and master plans report. Final FS &MP Report (vol. I), JPC & BAC/GKA JV

Republic of Kenya (2012a) Assessment of groundwater potential and hydrogeological survey report for 30 boreholes. Ministry of Water and Irrigation, District Water Officer, Lamu West District. LMU/DWO/046

Republic of Kenya (2012b) Draft of the national water policy. Minister for Water and Irrigation

Republic of Kenya (2013) Environmental and social impact assessment study report for construction of the first three berths of the proposed Lamu port and associated Infrastructure—final report. Ministry of Transport

Roeper T, Greskowiak J, Freund H, Massmann G (2013) Freshwater lens formation below juvenile dunes on a barrier island (Spiekeroog, Northwest Germany). Estuar Coast Shelf Sci 121:40–50

Saeed MM, Bruen M, Asghar MN (2002) A review of modelling approaches to simulate saline-upconing under skimming wells. Nord Hydrol 33:165–188

Schanze J, Truemper J, Burmeister C, Pavlik D, Kruhlov I (2012) A methodology for dealing with regional change in integrated water resources management. Environ Earth Sci 65:1405–1414

Schneider JC, Kruse SE (2005) Assessing selected natural and anthropogenic impacts on freshwater lens morphology on small barrier islands: dog Island and St. George Island, Florida, USA. Hydrogeol J 14(1–2):131–145

Scott PF (Eng) (2011) Geotechnical site investigations report for the proposed custom jetty in Lamu, Kenya. Reported prepared by Britech Consulting Engineers Ltd. for Comarco Construction Company Ltd

Serrat-Capdevila A, Valdes JB, Perez JG, Baird K, Mata LJ, Maddock T III (2007) Modeling climate change impacts and uncertainty on the hydrology of a riparian system: the San Pedro Basin (Arizona/Sonora). J Hydrol 347:48–66

Soni AK, Pujari PR (2010) Ground water vis-a-vis sea water intrusion analysis for a part of limestone tract of Gujarat Coast, India. J Water Resour Prot 2:462–468

Soni AK, Pujari PR (2012) Sea-water intrusion studies for coastal aquifers: some points to ponder. Open Hydrol J 6((Suppl 1-M2)):24–30

Stoll S, Franssen HJH, Butts M, Kinzelbach W (2011) Analysis of the impact of climate change on groundwater related hydrological fluxes: a multi-model approach including different downscaling methods. Hydrol Earth Syst Sci 15:21–38

Thornthwaite CW (1948) An approach toward a rational classification of climate. Geogr Rev 38:55–94

Uddameri V, Singaraju S, Hernandez EA (2014) Impacts of sea-level rise and urbanization on groundwater availability and sustainability of coastal communities in semi-arid South Texas. Environ Earth Sci 71:2503–2515

Vacher HL (1988) Dupuit–Ghyben–Herzberg analysis of strip-island lenses. Geol Soc Am Bull 100:580–591

Vandenbohede A, Hinsby K, Courtens C, Lebbe L (2011) Flow and transport model of a polder area in the Belgian coastal plain: example of data integration. Hydrogeol J 19:1599–1615

Wegehenkel M, Kersebaum KC (2009) An assessment of the impact of climate change on evapotranspiration, groundwater recharge, and low-flow conditions in a mesoscale catchment in Northeast Germany. J Plant Nutr Soil Sci-Zeitschrift Fur Pflanzenernahrung Und Bodenkunde 172:737–744

Werner AD, Simmons CT (2009) Impact of sea-level rise on sea water intrusion in coastal aquifers. Ground Water 47:197–204

Werner AD, Jakovovic D, Simmons CT (2009) Experimental observations of saltwater up-coning. J Hydrol 373:230–241

Werner AD, Ward JD, Morgan LK, Simmons CT, Robinson NI, Teubner MD (2012) Vulnerability indicators of sea water intrusion. Ground Water 50:48–58

Wirojanagud P, Charbeneau RJ (1985) Saltwater upconing in unconfined aquifers. J Hydraul Eng 111:417–434

Xu CY, Singh VP (2001) Evaluation and generalization of temperature-based methods for calculating evaporation. Hydrol Process 15:305–319

Zektser IS, Loaiciga HA (1993) Groundwater fluxes in global hydrologic cycle: past, present, and future. J Hydrol 144:405–427

Zinyowera MC, Jallow BP et al (1998) In: Watson RT, Zinyowera MC, Moss RH (eds) The regional impacts of climate change: an assessment of vulnerability: A Special Report of IPCC Working Group II. Cambridge University Press: Cambridge, UK, p 517